Analyzing the Discovery Potential for Light Dark Matter

Eder Izaguirre,[*] Gordan Krnjaic,[†] Philip Schuster,[‡] and Natalia Toro[§]
Perimeter Institute for Theoretical Physics, Waterloo, ON N2L 2Y5, Canada
(Received 12 May 2015; published 15 December 2015)

In this Letter, we determine the present status of sub-GeV thermal dark matter annihilating through standard model mixing, with special emphasis on interactions through the vector portal. Within representative simple models, we carry out a complete and precise calculation of the dark matter abundance and of all available constraints. We also introduce a concise framework for comparing different experimental approaches, and use this comparison to identify important ranges of dark matter mass and couplings to better explore in future experiments. The requirement that dark matter be a thermal relic sets a sharp sensitivity target for terrestrial experiments, and so we highlight complementary experimental approaches that can decisively reach this milestone sensitivity over the entire sub-GeV mass range.

DOI: 10.1103/PhysRevLett.115.251301 PACS numbers: 95.35.+d, 12.60.-i

Introduction.—That dark matter (DM) is a thermal relic from the hot early Universe is an inspiring possibility that motivates nongravitational interactions between dark and ordinary matter. The canonical example involves a heavy particle interacting through the weak force (Weakly Interacting Massive Particles). This scenario has motivated searches for DM scattering in underground detectors, for DM annihilation in the cosmos, and for DM production in high-energy colliders. These efforts achieve broad and powerful sensitivity to DM with mass between a few GeV and the TeV scale.

A thermal origin is equally compelling—and, in simple models, predictive—even if DM is not a Weakly Interacting Massive Particle. DM with any mass from a MeV to tens of TeVs can achieve the correct relic abundance by annihilating directly into standard model (SM) matter. However, the lower half of this mass range cannot be fully explored using existing strategies—an unfortunate situation that jeopardizes the legacy of the DM search effort. In particular, DM-nuclear and DM-electron scattering searches lose sensitivity precipitously for DM lighter than a few GeV or DM that scatters inelastically; limits on DM annihilation at low temperatures [most notably from the cosmic microwave background (CMB)] are irrelevant to many scenarios, and missing energy searches at high-energy colliders are blind to the interactions responsible for the DM abundance.

In this Letter, we sharply quantify the challenge of testing sub-GeV thermal DM that annihilates through an s-channel mediator directly into SM states. This is done with the completeness and accuracy needed to guide ongoing and future experimental efforts, which to date is absent in the literature. We start by summarizing well-known annihilation mechanisms arising from dark-sector mixing with SM fields, define minimal models representative of each mechanism, and compute all relevant constraints, some of which are new. For the first time, we accurately and precisely compute the required coupling strength for these minimal models to realize the correct DM relic density, including all SM thresholds and resonances. We then introduce a novel framework to compare all existing constraints on these representative models—under conservative assumptions designed to reveal weaknesses in existing searches—to the milestone target sensitivity provided by thermal DM freeze-out. Finally, we identify a small set of "flagship" experiments with complementary sensitivity—using direct detection, B-factory monophoton, and fixed-target missing momentum strategies—that together can decisively test the simplest models of light DM annihilating through SM mixing with a light mediator [1–7].

GeV-scale dark matter.—Viable light thermal DM scenarios can be classified by the spins and masses of the DM and mediator, by whether the thermal abundance or a primordial asymmetry dominates the DM density, and by the mediator's interactions with both DM and SM matter. SM symmetries substantially restrict the latter interactions: vector mediators can mix with the photon or weakly gauge a SM global symmetry, while scalars can mix with the Higgs boson (or have axionlike couplings in extensions of the SM). Rare B-meson decays largely exclude the scalar mediator scenarios for sub-GeV thermal DM, a discussion which we defer to future work, so we focus here on the possibilities for DM coupled through a vector mediator.

One concrete example is a scalar QED model of DM, where the "dark photon" A' is massive with coupling $g_D \equiv \sqrt{4\pi\alpha_D}$ to scalar DM currents $\mathcal{J}^\mu_D = i\varphi^*\partial^\mu\varphi + \text{c.c.}$ The DM scalar φ and dark photon A' have masses m_φ and $m_{A'}$, respectively. The leading SM coupling to this dark sector allowed by symmetries is photon-A' kinetic mixing, $\mathcal{L}_{\text{mix}} = \epsilon F'^{\mu\nu}F_{\mu\nu}$, where F' and F are the A' and photon field strengths, respectively [8,9]. After diagonalizing away the kinetic mixing term, the low-energy Lagrangian that describes dark-visible interactions is

$$\mathcal{L}_{\rm int} = A'_\mu(\epsilon e \mathcal{J}^\mu_{\rm EM} + g_D \mathcal{J}^\mu_D), \quad (1)$$

where $\mathcal{J}^\mu_{\rm EM}$ is the SM electromagnetic current.

For this representative case, we can now ask what parameter ranges achieve the correct φ relic density. For $m_{A'} \gtrsim m_\varphi$, the rate of annihilations $\varphi\varphi^* \to \bar{f}f$ determines the relic density. Neglecting m_f/m_φ corrections, the tree-level annihilation cross section at relative velocity $v_{\rm rel} \ll c$ is

$$\sigma v_{\rm rel} = \frac{8\pi}{3} \frac{\epsilon^2 \alpha \alpha_D m_\varphi^2 v_{\rm rel}^2}{(m_{A'}^2 - 4m_\varphi^2)^2 + m_{A'}^2 \Gamma^2}, \quad (2)$$

where Γ is the A' width. In the limit $m_{A'} \gg m_\varphi, \Gamma$, this cross section depends on dark-sector parameters only through the DM mass m_φ and the dimensionless combination

$$y \equiv \epsilon^2 \alpha_D \left(\frac{m_\varphi}{m_{A'}}\right)^4, \quad (3)$$

so matching the φ relic abundance to the observed DM density essentially fixes y as a function of m_φ (models with larger y can give rise to a subdominant component of the DM). Of course, near the fine-tuned region $m_{A'} \approx 2m_\varphi$, the precise milestone differs from that inferred from Eq. (3). For a detailed discussion concerning the relic density computation, see the Supplemental Material [10].

Before comparing existing data to this milestone, we comment on obvious and important variants of the model above. First, the DM may be a fermion instead of a scalar. A Dirac fermion $\chi = (\chi_1, \chi_2^\dagger)$ (decomposed here into Weyl spinors) can couple to A' through vector and/or axial currents. The axial piece leads to velocity-suppressed p-wave annihilation with scaling similar to Eq. (2), while the vector current $\mathcal{J}^\mu_D = \chi_1^\dagger \bar{\sigma}^\mu \chi_1 - \chi_2^\dagger \bar{\sigma}^\mu \chi_2$ leads to s-wave annihilation, and typically dominates. For this reason, we shall focus on the pure vector coupling.

If the global symmetry under which $\chi_{1,2}$ have opposite charges is broken (e.g., by a Higgs field that gives mass to the A'), operators such as $\mathcal{L}_{\rm break} = \delta \chi_1 \chi_1$ yield mass eigenstates $\chi_\pm = 1/\sqrt{2}(\chi_1 \pm \chi_2)$ split in mass by δ, with off-diagonal A' couplings $\mathcal{L}_{\rm int} = A'_\mu \chi_+^\dagger \bar{\sigma}^\mu \chi_-$. This exemplifies the inelastic or pseudo-Dirac scenario [11]. Analogously inelastic interactions can also arise in the scalar case.

Finally, for either scalar or fermionic DM, its total abundance may be set by a primordial particle-antiparticle asymmetry that dominates over the thermal relic abundance [12]. In this case Eq. (2) sets a lower bound on the collective interaction strength so that the symmetric component is subdominant.

Each scenario above has a counterpart where A' couples to a global symmetry current of the SM (e.g., baryon minus lepton number), rather than via kinetic mixing. The results that follow rely mainly on A' coupling to electrons, and so apply equally well [with $O(1)$ corrections to the thermal relic curve] to these scenarios, unless A' gauges a symmetry under which electrons are neutral, such as $\mu - \tau$ number [13,14].

Existing data confronts light DM.—Returning to the representative scenarios with a vector mediator, we now assess how well they are constrained by current data. Figure 1 quantifies each constraint in the plane of $y \equiv \epsilon^2 \alpha_D (m_\varphi/m_{A'})^4$ vs m_φ (or similarly for a fermion χ). The reason for quantifying constraints in these variables is simple: the dimensionless variable y controls the thermal relic density in thermal models and CMB signals in asymmetric models (except in a fine-tuned resonance region $m_{A'} \approx 2m_{\chi(\varphi)}$), so these important milestones appear as lines in the y-m_φ plane. Direct detection rates are also proportional to y, while accelerator-based constraints can be written in terms of y times positive powers of α_D and $m_{\chi(\varphi)}/m_{A'}$, as explained in detail below. These are both bounded from above for the scenario of interest, where DM annihilation into A' pairs is forbidden—α_D by perturbativity constraints, and $m_{\chi(\varphi)}/m_{A'}$ by the kinematic threshold for the annihilation process (in this section, we further specialize to $m_{A'} > 2m_{\chi(\varphi)}$ where A' decays invisibly). Thus, limits on y obtained for large values of α_D and $m_{\chi(\varphi)}/m_{A'}$, as we will show here, are generally conservative, in the sense that they become stronger as either parameter decreases. This logic, elaborated in the Supplemental Material [10], has one important caveat illustrated in the bottom-right panel of Fig. 1: as the mass ratio is increased, some direct-production experiments get weaker in the region near the A' production threshold.

The discussion below assumes $m_{A'} > 2m_{\varphi(\chi)}$, where A' decays invisibly into $\varphi(\chi)$ pairs, but the same experiments also constrain $\varphi(\chi)$ production through a lighter off-shell A'. For more details of each constraint, see the Supplemental Material [10].

CMB: Although MeV-GeV DM annihilation freezes out before the era of recombination, residual annihilations can reionize hydrogen and distort the high-ℓ CMB power spectrum [19–23]. These data can be used to constrain the total power injected by DM annihilations [23], which scales as the DM annihilation cross section (hence proportional to y) and can be invariantly compared with the relic density target. Dirac-fermion DM annihilating through an s-channel A' (not shown in Fig. 1) is ruled out by Planck 2015 data [24], but the other scenarios in Fig. 1 remain viable. In particular, the pseudo-Dirac scenario is viable because the DM annihilation rate during the CMB epoch is sharply suppressed relative to its value at freeze-out; see the Supplemental Material [10] for a discussion.

Light degrees of freedom: There is also an indirect bound on light DM $\lesssim$10 MeV that remains in thermal equilibrium with SM radiation (but not neutrinos) during big bang nucleosynthesis [29]. This bound is depicted by the dotted gray vertical curve in Fig. 1 and is more model

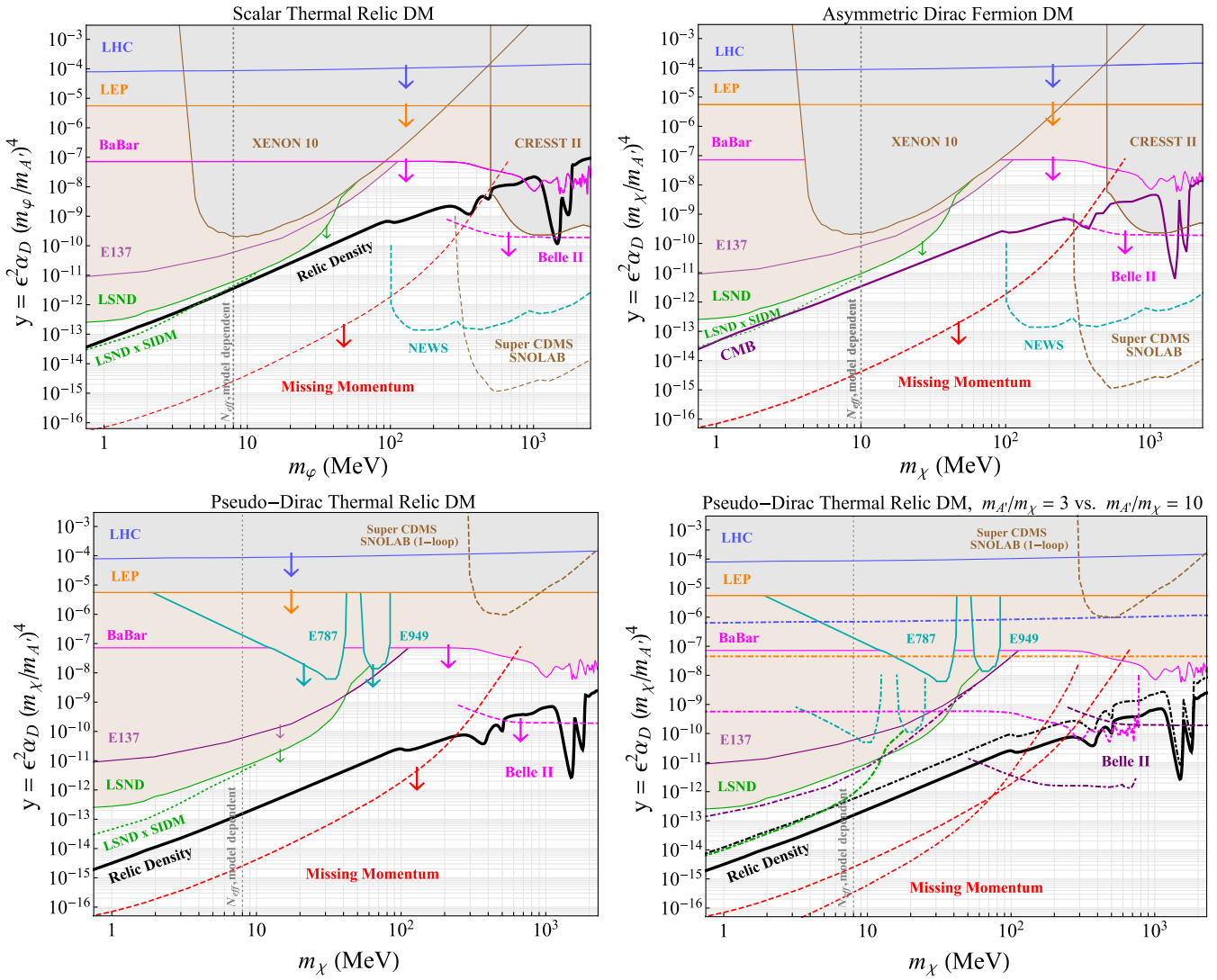

FIG. 1 (color online). Constraints and projections for representative vector-portal DM scenarios. For definiteness, we evaluate all constraints for $m_{\rm DM}/m_{A'} = 1/3$ and (except for the LSND × SIDM bound—see below) $\alpha_D = 0.5$, near the perturbativity limit. The relic density, CMB, and direct detection contours scale roughly as $\epsilon^2\alpha_D(m_{\rm DM}/m_{A'})^4$ (plotted on the y axis), and so are insensitive to separate factors in the above. For other constraints, this choice is conservative, in that smaller choices of α_D and/or $m_{\rm DM}/m_{A'}$ would shift the shaded regions downward (see text); arrows denote the shift in sensitivity for $\alpha_D \to 0.05$. We illustrate these constraints for (top left) scalar elastic-scattering thermal relic DM, (top right) asymmetric Dirac-fermion DM, and (bottom left) pseudo-Dirac or inelastic fermion thermal-relic DM, with splitting $\delta \gtrsim 100$ keV. Dirac-fermion thermal-relic DM is fully excluded by the CMB constraint and inelastic or asymmetric scalar DM is quite similar to the right panel, but with CMB and direct detection constraints weakened. CMB, self-interaction (SIDM), and direct detection constraints all depend on the $\chi(\varphi)$ abundance, and are computed assuming the full DM abundance, not the thermal abundance expected for given masses and couplings. In all plots, gray shaded regions (color online) represent traditional DM constraints (e.g., direct detection), while nontraditional accelerator probes are shaded beige. We note that pseudo-Dirac limits are modified (and new dedicated searches are possible [15]) if δ is large enough that χ_+ can decay on detector length scales. Bottom right: pseudo-Dirac DM parameter space and future projections for $m_{\rm DM}/m_{A'} = 1/3$ (solid curves) and $1/10$ (dot dashed). A detailed discussion of these constraints and their scaling with y can be found in the Supplemental Material [10], which contains Refs. [16–49].

dependent than accelerator probes because it can be evaded with additional sources of dark sector radiation (e.g., sterile neutrinos).

Direct detection: Elastic DM-nuclear interactions are constrained by recent results from CRESST [32], whose low threshold allows for sensitivity down to a few hundreds of MeVs in DM mass. For masses below the CRESST threshold, DM-electron scattering is constrained by XENON10 ionization data [31,50]. Since the nonrelativistic DM-SM scattering cross section is proportional to the y variable, the constraints presented in Fig. 1 are invariant under different assumptions about α_D and $m_{A'}/m_\chi$; see the

Supplemental Material [10] for a discussion. For pseudo-Dirac DM (Fig. 1, top left), tree-level scattering is inelastic and kinematically forbidden for mass splittings of order $\delta \gtrsim$ keV; elastic scattering arises from a one-loop box diagram, which scales as y^2 and is also invariant on the y vs m_χ plane.

B factories: Light DM can be constrained using monophoton and missing-energy production at B factories. The *BABAR* search for an (untagged) $\Upsilon(3S) \to \gamma +$ invisible [35] constrains the process $e^+e^- \to \gamma + A'^{(*)} \to \gamma\chi\bar{\chi}$ [33,34]. Since the A' production rate only depends on ϵ and the beam energy, we conservatively choose $m_\varphi/m_{A'} = 1/3$ and $\alpha_D = 1/2$ to build the variable using these data; smaller choices of either quantity would overstate the *BABAR* constraint.

High energy colliders: Electroweak precision tests at LEP constrain the existence of a new massive photon. In particular, kinetic mixing induces a shift in the mass of the Z^0 boson, and the constraint depends on ϵ and only mildly on $m_{A'}$ [37,38]. At the LHC, light DM can be produced in association with a QCD jet. Recasting a CMS DM search [51] in the monojet and missing energy channel places a constraint on the y vs m_χ plane. These constraints do not scale with y so we adopt the benchmark $m_\varphi/m_{A'} = 1/3$ and $\alpha_D = 1/2$ in constructing y for colliders.

Beam-dump experiments: Fixed-target beam dump experiments offer another powerful probe of light DM. A reinterpretation of LSND's measurement of the electron-neutrino neutral current cross section [41] sets the strongest constraints for masses below 100 MeV [39,52–54]. In this setup rare neutral pion decays through the vector portal produce the A', which decay to yield a DM beam. This beam scatters in a downstream detector and the rate for this process is constrained by LSND electron recoil data. Similarly, the electron beam-dump experiment E137 offers complementary sensitivity to the A' produced radiatively in fixed-target electron beam dump interactions. Once produced, the A' decay to boosted DM pairs, which can scatter in a downstream detector [45]. The null results of Ref. [44] place a bound on the DM-electron interaction rate. For both experiments, the production yield scales with couplings as ϵ^2 and the detection probability as $\epsilon^2\alpha_D$, so that overall yield scales as $\epsilon^4\alpha_D$. The benchmark $\alpha_D = 1/2$ yields a conservative bound on y that improves as $1/\sqrt{\alpha_D}$ for smaller α_D. The $m_{A'}$ dependence of these experiments' yields is more complex, but again the choice $m_\varphi/m_{A'} = 1/3$ is conservative, with stronger constraints for smaller ratios.

DM self-interactions: Constraints from the Bullet Cluster and from cluster lensing [42,43] bound the DM-DM self-interaction cross section. This, in turn, constrains α_D at low mass and rules out the benchmark conservative choice $\alpha_D = 1/2$ for a DM/mediator mass ratio of $1/3$ in the region where LSND dominates other experiments. To account for this constraint, we show a dotted green curve in Fig. 1 that uses the α_D inferred from self-interaction bounds instead.

Supernovae: The production of any free-streaming $\bar{\chi}\chi$ pairs inside supernovae (SN) is constrained by observations of SN 1987A [46,47]. As discussed in Ref. [48], the SN core luminosity can be appreciable, but the scattering of χ off baryons can be large enough for the χ diffusion escape time to fall below a few seconds.

Visibly decaying mediators: If $m_{A'} < 2m_{\varphi(\chi)}$, the A' signals at colliders are quite rich—the accelerator-based constraints discussed above have counterparts proceeding through an off-shell A', and searches for visible decays $A' \to \ell^+\ell^-$ become quite powerful. Numerous experiments [5,44,55–67] constrain this parameter space, and several more are expected to run in the next few years [68–73]. These results and new experiments are summarized in Ref. [74]. The interplay of these constraints is illustrated in Fig. 2 for inelastic fermion DM with representative parameter choices $m_{A'} = 1.1m_\chi$ and $\alpha_D = 0.5$. The situation is qualitatively similar for the scalar and asymmetric DM scenarios.

The status and future of light DM science.—Present status: While scalar mediated light DM scattering is tightly constrained by meson decay, vector mediated scattering is viable over a wide range of mass and couplings. Figures 1 and 2 illustrate that current experiments are several orders of magnitude away from decisively testing thermal vector-portal dark matter. Electron-scattering limits are 2–3 orders of magnitude short of the thermal target even at the optimal DM masses for these experiments; CMB energy injection bounds exclude the thermal target for symmetric Dirac-fermion DM, but are far from constraining pseudo-Dirac, asymmetric, and scalar DM scenarios. Low-energy accelerator-based experiments have made significant progress exploring this parameter space—*BABAR* data do robustly exclude scalar vector-portal DM with few-GeV mass—but they too leave 2–4 orders of magnitude of unexplored parameter space below a GeV.

Future probes with existing strategies: Progress searching for light DM based on existing experimental strategies will be driven by three fronts: direct detection, B factories, and fixed-target experiments. Direct detection through electron scattering is currently background limited; future improvements depend on this relatively new field's success in pushing experimental thresholds to lower energies and minimizing backgrounds [31,50]. In parallel, nuclear-recoil direct detection experiments are expected to lower their target masses and recoil energy thresholds enough to start exploring the sub-GeV region [49,76,77]. Especially promising are projections from the SuperCDMS SNOLAB [49] and NEWS experiments [78] shown in Fig. 1. Belle II, an upcoming high-luminosity B factory in Japan, can also significantly improve on current B factory sensitivity to light DM if it is instrumented with a monophoton trigger [34]. Together, these experiments can

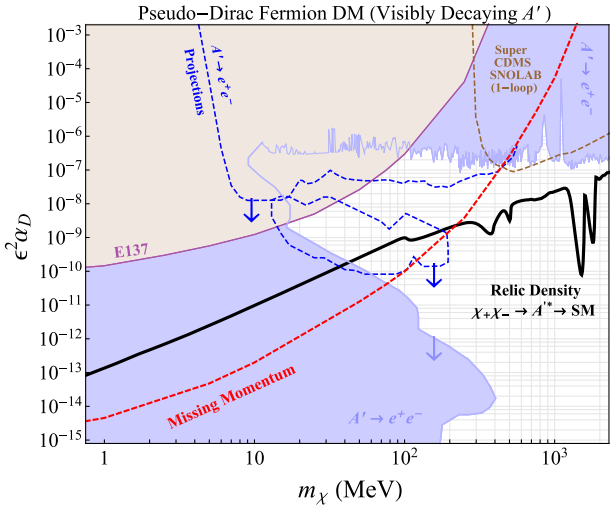

FIG. 2 (color online). Same as Fig 1, but assuming $m_{A'} = 1.1m_\chi$, where the relic abundance is still achieved through s-channel annihilation, but A' decays visibly. Dashed blue contours show projected sensitivities from Ref. [74] for future $A' \to \ell^+\ell^-$ searches in the next few years. Depending on the χ and A' masses, models below the relic density line may still achieve viable thermal abundances through other processes—see Ref. [75].

explore the viable thermal light DM parameter space above 250–400 MeV. Fixed-target beam-dump experiments hold significant promise to probe the lighter end of this range: future neutrino facilities can extend the sensitivity for DM below the pion threshold [40], while future electron beam dumps with relatively small forward detectors extending the sensitivity for $m_\chi \gtrsim m_\pi/2$ [33,79]. The fixed-target program to search for visibly decaying mediators, summarized in Ref. [74], will play an important role in testing the intermediate-mass scenario shown in Fig. 2.

Fixed-target missing momentum concept: A particularly powerful probe of vector-portal light DM is to search for missing momentum in electron-nucleus fixed target collisions [48,80], based on the observation that most of the beam energy in processes $eN \to eNA', A' \to \bar{\chi}\chi$ (and similarly for off-shell A') is typically carried by the invisible $\bar{\chi}\chi$ pair. Such experiments' signal rate scales as $\propto \epsilon^2$ (as opposed to ϵ^4 for beam-dump searches). The authors have argued in Ref. [48] that such an experiment can suppress backgrounds to <1 event in 10^{16} electrons on target, provided the detector is capable of measuring the recoiling electron's transverse momentum and vetoing products of rare photonuclear reactions. Figures 1 and 2 illustrate the significant potential of this approach. The dashed red curves show 2.3 event yields for 3×10^{16} electrons incident on a thin tungsten target; see the Supplemental Material [10] for more details.

Scenarios without a thermal-relic milestone: For DM heavier than the mediator, t-channel annihilation into two mediators typically dominates over the s-channel processes used to compute the "relic density" curve in Figs. 1 and 2. For scalar DM and/or vector mediators, this process is never p-wave suppressed, and in the inelastic scenario it allows two of the lighter χ_- particles to annihilate one another—thus, thermal DM models of these types are inconsistent with the CMB constraint. However, there are several scenarios compatible with the CMB where annihilation into two mediators dominates: annihilation of fermion DM into scalar mediators (p wave), annihilation into vector mediators heavier than the DM (relying on the Boltzmann tail [75]), and asymmetric DM. The thermal relic abundance cannot be used to predict a lower bound on y in these cases. A more appropriate figure of merit than y for comparing direct detection and accelerator-based experiments for $m_{A'} < m_{\varphi(\chi)}$ is $\alpha\alpha_D\epsilon^2$ (or similarly for scalar mediators), where the direct detection limits are evaluated conservatively for $m_{A'} \approx m_{\varphi(\chi)}$.

Summary: This Letter shows that many of the simplest models for sub-GeV thermal DM are consistent with all current data. A generic and simple possibility is that DM couples to the SM through a kinetically mixed dark photon. Although symmetric Dirac-fermion DM annihilating through the vector portal is excluded by CMB limits, scalar, pseudo-Dirac, and asymmetric DM scenarios are all largely untested. These scenarios define sharp milestones for future experiments to reach. Together, planned B factories (Belle-II, if equipped with a monophoton trigger), direct detection experiments (Super-CDMS, NEWS, and other efforts), and possible electron fixed-target experiments based on missing momentum should be capable of robustly reaching this target over almost all of the MeV-to-GeV mass range.

We thank Wolfgang Altmanshoffer, Rouven Essig, Mariana Gonzalez, Valentin Hirshi, Yoni Kahn, David Morrissey, Maxim Pospelov, Joshua Ruderman, Tracy Slatyer, and Kathryn Zurek for helpful conversations. This research was supported in part by Perimeter Institute for Theoretical Physics. Research at Perimeter Institute is supported by the Government of Canada through Industry Canada and by the Province of Ontario through the Ministry of Research and Innovation.

*eizaguirre@perimeterinstitute.ca
†gkrnjaic@perimeterinstitute.ca
‡pschuster@perimeterinstitute.ca
§ntoro@perimeterinstitute.ca

[1] B. W. Lee and S. Weinberg, Phys. Rev. Lett. **39**, 165 (1977).
[2] C. Boehm, T. Ensslin, and J. Silk, J. Phys. G **30**, 279 (2004).
[3] C. Boehm and P. Fayet, Nucl. Phys. **B683**, 219 (2004).
[4] M. Pospelov, A. Ritz, and M. B. Voloshin, Phys. Lett. B **662**, 53 (2008).
[5] M. Pospelov, Phys. Rev. D **80**, 095002 (2009).
[6] N. Arkani-Hamed, D. P. Finkbeiner, T. R. Slatyer, and N. Weiner, Phys. Rev. D **79**, 015014 (2009).

[7] M. Pospelov and A. Ritz, Phys. Lett. B **671**, 391 (2009).
[8] L. Okun, Sov. Phys. JETP **56**, 502 (1982).
[9] B. Holdom, Phys. Lett. **166B**, 196 (1986).
[10] See Supplemental Material at http://link.aps.org/supplemental/10.1103/PhysRevLett.115.251301 for detailed description of the calculations and constraints presented in this Letter.
[11] D. Smith and N. Weiner, Phys. Rev. D **64**, 043502 (2001).
[12] K. M. Zurek, Phys. Rep., **537**, 91 (2014).
[13] W. Altmannshofer, S. Gori, M. Pospelov, and I. Yavin, Phys. Rev. D **89**, 095033 (2014).
[14] W. Altmannshofer, S. Gori, M. Pospelov, and I. Yavin, Phys. Rev. Lett. **113**, 091801 (2014).
[15] E. Izaguirre, G. Krnjaic, P. Schuster, and N. Toro (to be published).
[16] E. W. Kolb and M. S. Turner, Front. Phys. **69**, 1 (1990).
[17] K. A. Olive *et al.* (Particle Data Group), Chin. Phys. C **38**, 090001 (2014).
[18] P. Gondolo and G. Gelmini, Nucl. Phys. **B360**, 145 (1991).
[19] D. P. Finkbeiner, S. Galli, T. Lin, and T. R. Slatyer, Phys. Rev. D **85**, 043522 (2012).
[20] T. Lin, H.-B. Yu, and K. M. Zurek, Phys. Rev. D **85**, 063503 (2012).
[21] S. Galli, F. Iocco, G. Bertone, and A. Melchiorri, Phys. Rev. D **84**, 027302 (2011).
[22] M. S. Madhavacheril, N. Sehgal, and T. R. Slatyer, Phys. Rev. D **89**, 103508 (2014).
[23] P. Ade *et al.* (Planck), Astron. Astrophys. **571**, A16 (2014).
[24] P. A. R. Ade *et al.* (Planck), arXiv:1502.01589.
[25] J. Hisano, M. Kawasaki, K. Kohri, and K. Nakayama, Phys. Rev. D **79**, 063514 (2009).
[26] J. Hisano, M. Kawasaki, K. Kohri, T. Moroi, and K. Nakayama, Phys. Rev. D **79**, 083522 (2009).
[27] K. Jedamzik and M. Pospelov, New J. Phys. **11**, 105028 (2009).
[28] B. Henning and H. Murayama, arXiv:1205.6479.
[29] K. M. Nollett and G. Steigman, Phys. Rev. D **89**, 083508 (2014).
[30] C. Boehm, M. J. Dolan, and C. McCabe, J. Cosmol. Astropart. Phys. 08 (2013) 041.
[31] R. Essig, A. Manalaysay, J. Mardon, P. Sorensen, and T. Volansky, Phys. Rev. Lett. **109**, 021301 (2012).
[32] G. Angloher *et al.* (CRESST), arXiv:1509.01515.
[33] E. Izaguirre, G. Krnjaic, P. Schuster, and N. Toro, Phys. Rev. D **88**, 114015 (2013).
[34] R. Essig, J. Mardon, M. Papucci, T. Volansky, and Y.-M. Zhong, J. High Energy Phys. 11 (2013) 167.
[35] B. Aubert *et al.* (*BABAR* Collaboration), arXiv:0808.0017.
[36] H. Davoudiasl and W. J. Marciano, Phys. Rev. D **92**, 035008 (2015).
[37] A. Hook, E. Izaguirre, and J. G. Wacker, Adv. High Energy Phys. **2011**, 1 (2011).
[38] D. Curtin, R. Essig, S. Gori, and J. Shelton, J. High Energy Phys. 02 (2015) 157.
[39] P. deNiverville, M. Pospelov, and A. Ritz, Phys. Rev. D **84**, 075020 (2011).
[40] Y. Kahn, G. Krnjaic, J. Thaler, and M. Toups, Phys. Rev. D **91**, 055006 (2015).
[41] L. Auerbach *et al.* (LSND), Phys. Rev. D **63**, 112001 (2001).
[42] M. Markevitch, A. H. Gonzalez, D. Clowe, A. Vikhlinin, W. Forman, C. Jones, S. Murray, and W. Tucker, Astrophys. J. **606**, 819 (2004).
[43] J. Miralda-Escude, Astrophys. J. **564**, 60 (2002).
[44] J. D. Bjorken, S. Ecklund, W. R. Nelson, A. Abashian, C. Church, B. Lu, L. W. Mo, T. A. Nunamaker, and P. Rassmann, Phys. Rev. D **38**, 3375 (1988).
[45] B. Batell, R. Essig, and Z. Surujon, Phys. Rev. Lett. **113**, 171802 (2014).
[46] R. Bionta, G. Blewitt, C. Bratton, D. Casper, A. Ciocio *et al.*, Phys. Rev. Lett. **58**, 1494 (1987).
[47] K. Hirata *et al.* (Kamiokande-II), Phys. Rev. Lett. **58**, 1490 (1987).
[48] E. Izaguirre, G. Krnjaic, P. Schuster, and N. Toro, Phys. Rev. D **91**, 094026 (2015).
[49] P. Cushman *et al.*, in Community Summer Study 2013: Snowmass on the Mississippi (CSS2013) Minneapolis, MN, USA, July 29-August 6, 2013, 2013.
[50] R. Essig, J. Mardon, and T. Volansky, Phys. Rev. D **85**, 076007 (2012).
[51] V. Khachatryan *et al.* (CMS Collaboration), Eur. Phys. J. C **75**, 235 (2015).
[52] B. Batell, M. Pospelov, and A. Ritz, Phys. Rev. D **80**, 095024 (2009).
[53] P. deNiverville, D. McKeen, and A. Ritz, Phys. Rev. D **86**, 035022 (2012).
[54] B. A. Dobrescu and C. Frugiuele, Phys. Rev. Lett. **113**, 061801 (2014).
[55] E. Riordan, M. Krasny, K. Lang, P. De Barbaro, A. Bodek *et al.*, Phys. Rev. Lett. **59**, 755 (1987).
[56] A. Bross, M. Crisler, S. H. Pordes, J. Volk, S. Errede, and J. Wrbanek, Phys. Rev. Lett. **67**, 2942 (1991).
[57] H. Davoudiasl, H.-S. Lee, and W. J. Marciano, Phys. Rev. D **86**, 095009 (2012).
[58] M. Endo, K. Hamaguchi, and G. Mishima, Phys. Rev. D **86**, 095029 (2012).
[59] D. Babusci *et al.* (KLOE-2 Collaboration), Phys. Lett. B **720**, 111 (2013).
[60] P. Adlarson *et al.* (WASA-at-COSY Collaboration), Phys. Lett. B **726**, 187 (2013).
[61] S. Abrahamyan *et al.* (APEX Collaboration), Phys. Rev. Lett. **107**, 191804 (2011).
[62] H. Merkel *et al.* (A1 Collaboration), Phys. Rev. Lett. **106**, 251802 (2011).
[63] J. D. Bjorken, R. Essig, P. Schuster, and N. Toro, Phys. Rev. D **80**, 075018 (2009).
[64] M. Reece and L.-T. Wang, J. High Energy Phys. 07 (2009) 051.
[65] B. Aubert *et al.* (*BABAR* Collaboration), Phys. Rev. Lett. **103**, 081803 (2009).
[66] J. B. Dent, F. Ferrer, and L. M. Krauss, arXiv:1201.2683.
[67] H. K. Dreiner, J.-F. Fortin, C. Hanhart, and L. Ubaldi, Phys. Rev. D **89**, 105015 (2014).
[68] R. Essig, P. Schuster, N. Toro, and B. Wojtsekhowski, J. High Energy Phys. 02 (2011) 009.
[69] M. Battaglieri, S. Boyarinov, S. Bueltmann, V. Burkert, A. Celentano *et al.*, Nucl. Instrum. Methods Phys. Res., Sect. A **777**, 91 (2015).
[70] M. Freytsis, G. Ovanesyan, and J. Thaler, J. High Energy Phys. 01 (2010) 111.

[71] B. Wojtsekhowski, AIP Conf. Proc. **1160**, 149 (2009).
[72] B. Wojtsekhowski, D. Nikolenko, and I. Rachek, arXiv:1207.5089.
[73] T. Beranek, H. Merkel, and M. Vanderhaeghen, Phys. Rev. D **88**, 015032 (2013).
[74] R. Essig, J. A. Jaros, W. Wester, P. H. Adrian, S. Andreas *et al.*, arXiv:1311.0029.
[75] R. T. D'Agnolo and J. Ruderman (to be published).
[76] A. Chavarria, J. Tiffenberg, A. Aguilar-Arevalo, D. Amidei, X. Bertou *et al.*, Phys. Procedia **61**, 21 (2015).
[77] G. Gerbier, I. Giomataris, P. Magnier, A. Dastgheibi, M. Gros *et al.*, arXiv:1401.7902.
[78] S. Profumo, arXiv:1507.07531.
[79] E. Izaguirre, G. Krnjaic, P. Schuster, and N. Toro, Phys. Rev. D **90**, 014052 (2014).
[80] S. Andreas, S. Donskov, P. Crivelli, A. Gardikiotis, S. Gninenko *et al.*, Phys. Rev. D **89**, 075008 (2014).